Supplemental Data

Death receptors 4 and 5 activate Nox1 NADPH oxidase through riboflavin kinase to induce reactive oxygen species-mediated apoptotic cell death

Kyung-Jin Park, Chang-Han Lee, Aeyung Kim, Ki Jun Jeong, Chul-Ho Kim, and Yong-Sung Kim

Inventory of Supplemental Data

Supplemental Data : six supplementary Figures

- Fig. S1 is associated with Fig. 1.
- Fig. S2 is associated with Fig. 2.
- Fig. S3 is associated with Fig. 3.
- Fig. S4 is associated with Figs. 3. & 5.
- Fig. S5 is associated with Fig. 4.
- Fig. S6 is associated with Fig. 6.

Supplemental Experimental Procedures,
Supplemental References

Figure S1

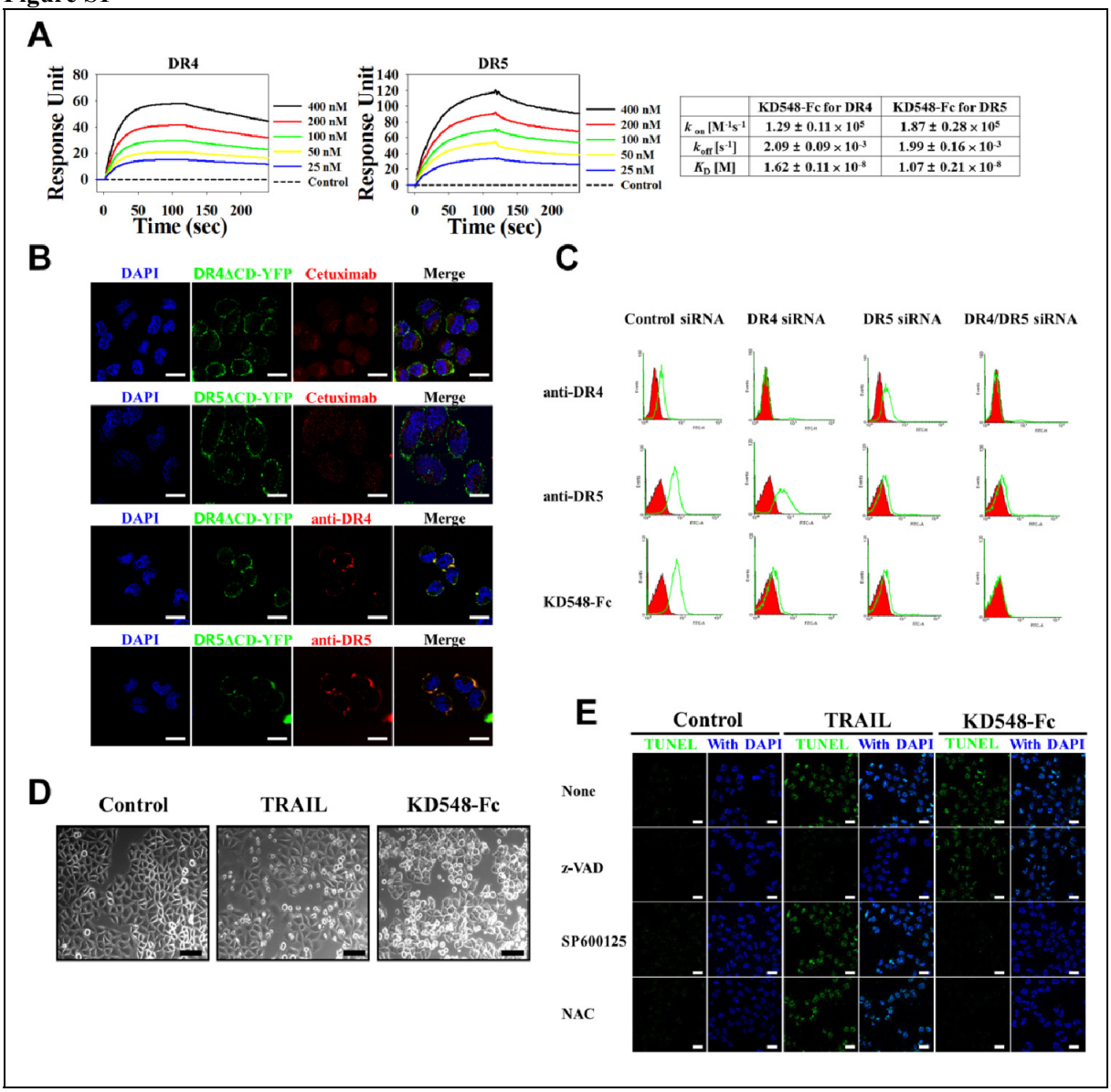

Figure S1. KD548-Fc induces apoptotic cell death by specific engagement of DR4 and/or DR5 in HeLa cells.

(A) Kinetic interactions of KD548-Fc with the extracellular domains of DR4 and DR5 determined by SPR analyses. SPR sensograms were obtained from injections of serially diluted KD548-Fc at 400, 200, 100, 50, and 25 nM over the DR4 or DR5 immobilized surface at 400 response units. The bottom line (dotted line) indicates no binding activity of KD548-Fc (400 nM) to a negative control of BSA.

(B) Binding activity of anti-EGFR Cetuximab (negative control), anti-DR4 or -DR5 mAb (positive control) for cell surface expressed DR5 and DR4. TRITC-labeled Cetuximab (1 μg/ml), anti-DR4 or -DR5 mAb (1 μg/ml) was incubated for 30 min at 4°C with HeLa cells transiently transfected with DR4ΔCD-YFP and DR5ΔCD-YFP. Nuclei were costained with DAPI. Bar, 20 μm. Cetuximab against epidermal growth factor receptor (EGFR) did not show any colocalization with DR4 or DR5.

(C) Specific binding activity of KD548-Fc for the cell surface-expressed DR4 and DR5. FITC-labeled KD548-Fc (1 μM) or anti-DR4 or -DR5 mAb (1 μg/ml) was incubated for 30 min at 4°C with HeLa cells transiently transfected with the indicated siRNA for 36 hr. Then the binding levels were analyzed by flow cytometry. DR4/DR5 siRNA indicates the cotransfection of DR4 and DR5 siRNAs. Red fill, cells only; green line, protein-labeled cells.
(D) Representative phase contrast microscopic images of HeLa cells, left untreated (control) or treated with either TRAIL (30 nM) or KD548-Fc (0.8 μM) for 20 hr. Bar, 40 μm.
(E) Apoptosis was evaluated by TUNEL staining. Cells pretreated with the indicated chemicals for 1 hr were further left untreated (control), or treated with TRAIL (30 nM) or KD548-Fc (0.8 μM) for 20 hr prior to TUNEL staining. Left, TUNEL staining; Right, merged with DAPI (nuclei) staining.

Figure S2

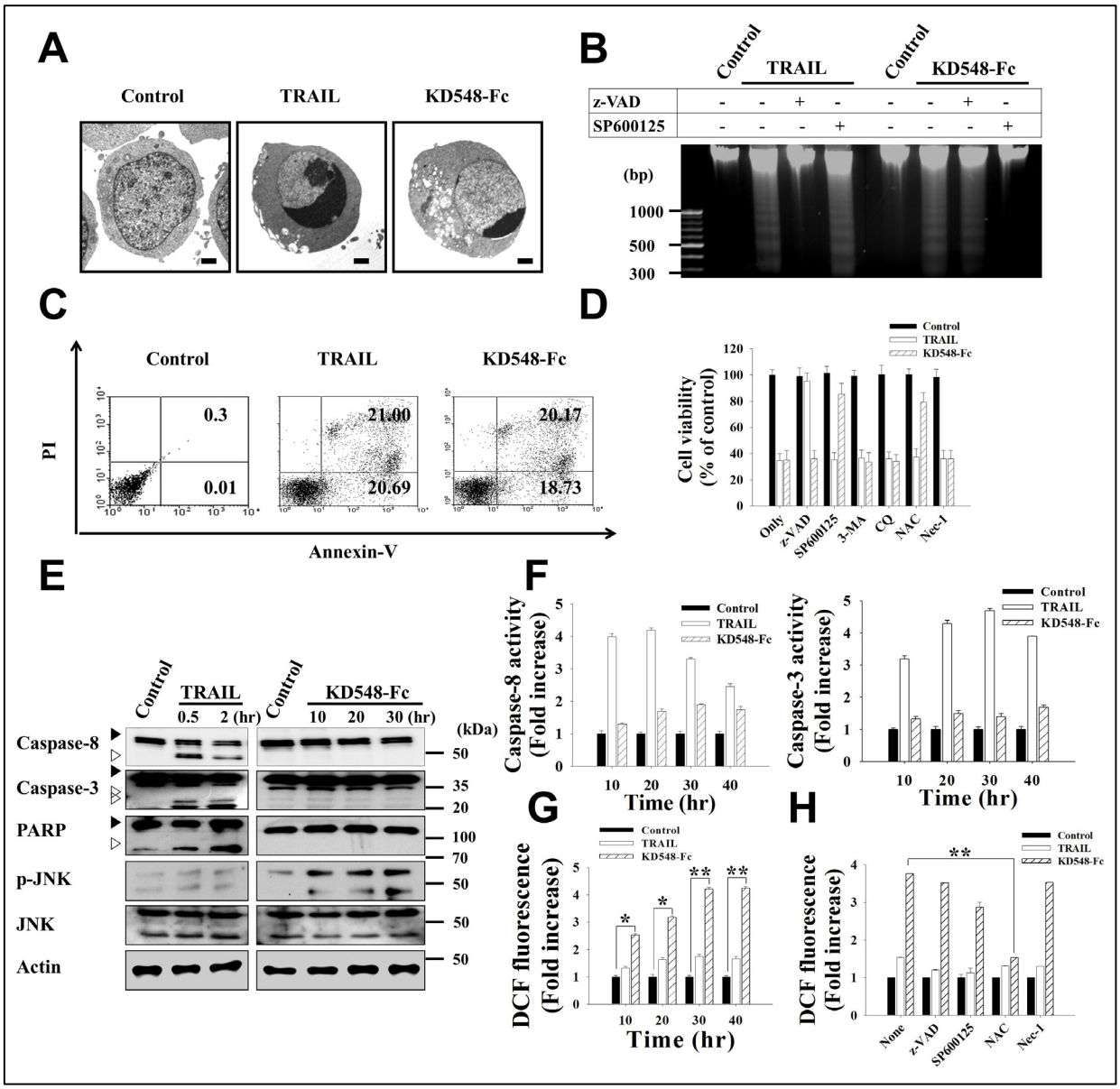

Figure S2. KD548-Fc-induced apoptotic cell death is dependent on ROS generation and JNK activation, but not caspase activation, in Jurkat cells.

(A) Representative TEM images of Jurkat cells, which were left untreated (control), or treated with either TRAIL (30 nM) for 3 hr or KD548-Fc (0.8 μM) for 20 hr. Bar, 2 μm.

(B) Oligonucleosomal DNA fragmentation assay for Jurkat cells, pretreated for 1 h with z-VAD (10 μM) or SP600125 (10 μM) and further incubated with TRAIL (30 nM) for 6 hr or KD548-Fc (0.8 μM) for 48 hr. 'Control' means untreated cells.

(C) Dual staining of Annexin V-FITC and PI for Jurkat cells left untreated for 30 hr (control) or treated with either TRAIL (30 nM) for 3 hr or KD548-Fc (0.8 μM) for 30 hr. Samples were then analyzed by flow cytometry. Annexin V-FITC$^+$/PI$^-$ cells (bottom right quadrant, % shown) and Annexin V-FITC$^+$/PI$^+$ cells (top right quadrant, % shown) are considered as "early apoptotic" and "dead" cells,

respectively.
(D) Effects of pharmacological inhibitors on the cell death of Jurkat cells treated with either KD548-Fc or TRAIL. Cells pretreated for 1 hr with the indicated pharmacological inhibitor were further incubated with TRAIL (30 nM) or KD548-Fc (0.8 μM) for 40 hr prior to the determination of cell viability by MTT assay.
(E) Western blots analysis of caspase-8, -3, PARP, JNK activations by treatment of TRAIL or KD548-Fc. Jurkat cells were treated with either TRAIL (30 nM) or KD548-Fc (0.8 μM) for the indicated periods prior to Western blots.
(F) Caspase-8 and -3 activity assay in response to TRAIL or KD548-Fc. Jurkat cells were treated TRAIL (30 nM) or KD548-Fc (0.8 μM) for the indicated periods and then activated caspase-8 (left) and caspase-3 (right) was detected using the respective fluorogenic substrates and then flow cytometry.
(G) ROS production in the cells, left untreated (control), or treated with TRAIL or KD548-Fc for the indicated periods.
(H) Effects of pharmacological inhibitors on the KD548-Fc-induced ROS production in the cells, pretreated for 1 hr with the indicated pharmacological inhibitor and then left untreated (control), or treated with TRAIL (30 nM) or KD548-Fc (0.8 μM) for 20 hr.
(D, F, G, and H) Data represent mean ± SEM of three independent experiments carried out in triplicate. (G and H) *, $P < 0.05$; **, $P < 0.001$ compared with the corresponding control.

Figure S3

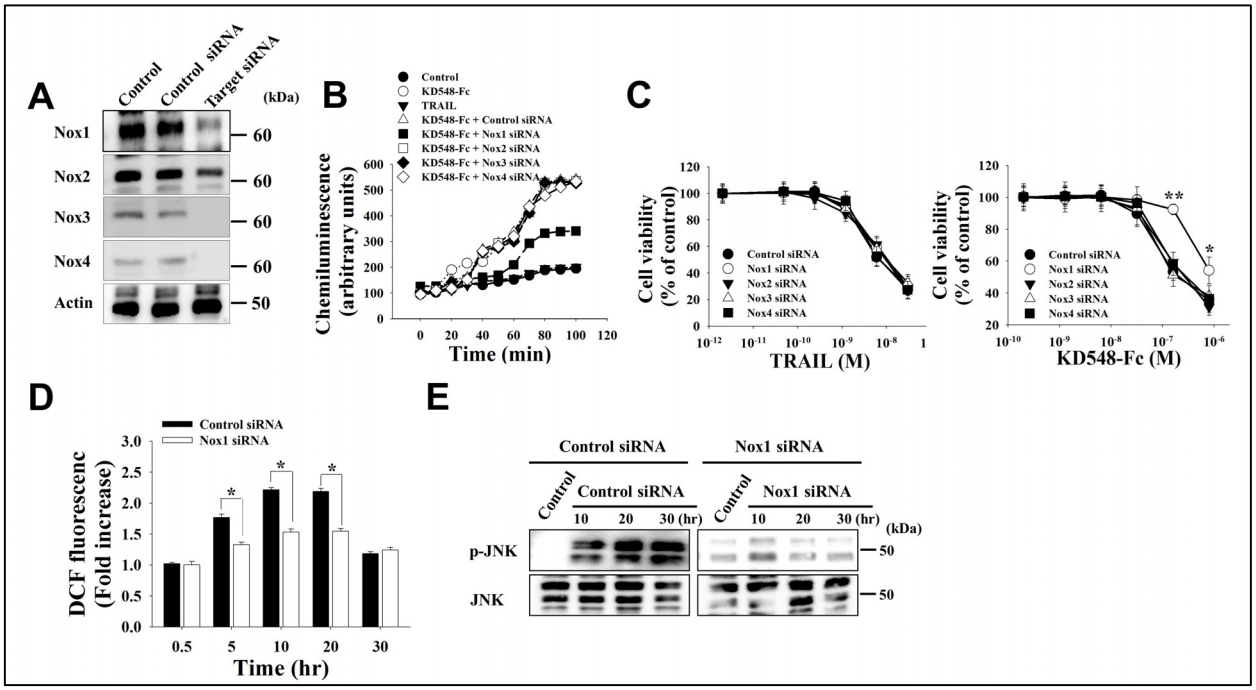

Figure S3. KD548-Fc activates Nox1 NADPH oxidase to produce superoxide anion, leading to intracellular ROS accumulation, sustained JNK activation and eventually apoptotic cell death in HCT116 cells.

(A) Western blots showing the knockdown of Nox1, Nox2, Nox3 or Nox4 expression by siRNA transfection into HCT116 cells. 'Control' means untransfected cells. Molecular size markers are shown on the right in kDa.

(B, C) Effects of knockdown of Nox1, Nox2, Nox3 or Nox4 on superoxide anion generation (B) and cell viability (C) in the cells, left untreated (control) or treated with KD548-Fc (B, C), or treated with TRAIL (C). (B) Cells were treated with 0.8 μM of KD548-Fc. The data are representative of three separate experiments with the same results. (C) Cells transfected with siRNA for 36 hr were further incubated with the indicated concentrations of KD548-Fc or TRAIL for 40 hr.

(D, E) Effect of Nox1 knockdown on ROS production (D) or JNK phosphorylation (E) in the cells, untreated (control) or treated with KD548-Fc (0.8 μM) for the indicated periods.

(C, D) Data represent mean ± SEM of three independent experiments carried out in triplicate. *, P <0.05; **, P <0.001 compared with the cells transfected with control siRNA.

Figure S4

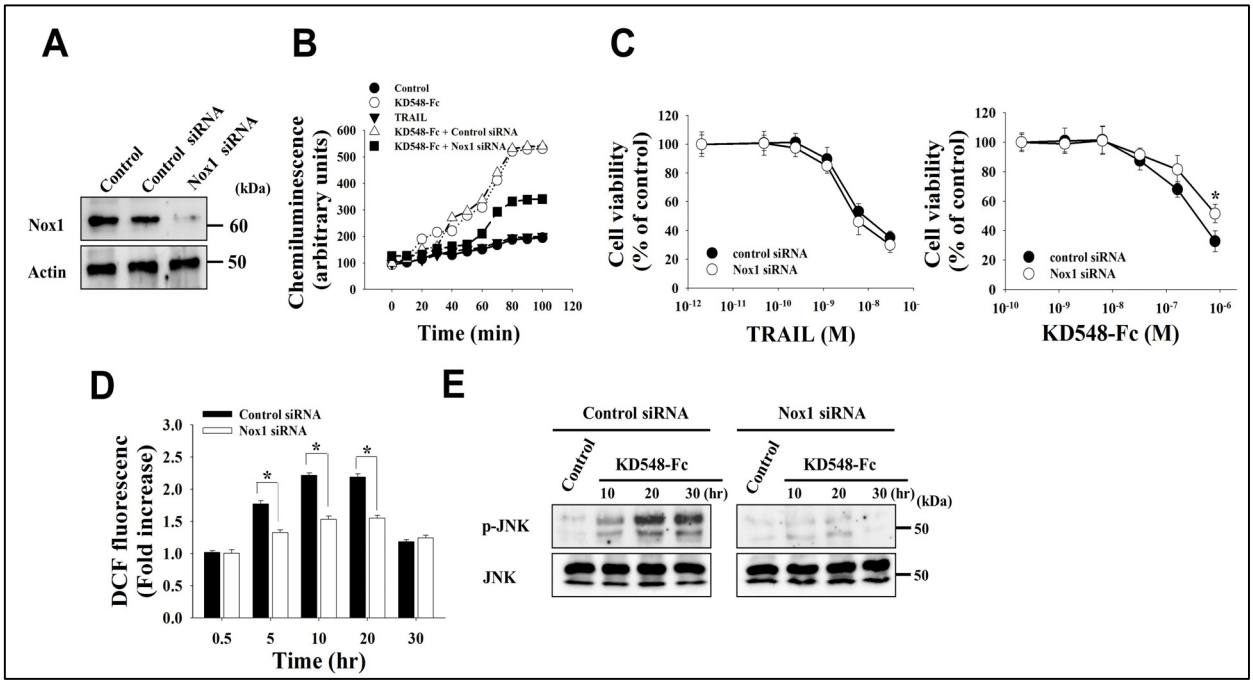

Figure S4. Knockdown of Nox1 NADPH oxidase inhibits the KD548-Fc-induced superoxide anion production, ROS generation, sustained JNK activation and cell death in Jurkat cells.
(A) Western blots showing Nox1 expression in the cells, untransfected (control) or transfected with the indicated siRNA for 36 hr. Molecular size markers are shown on the right in kDa.
(B-E) Effect of Nox1 knockdown on the superoxide anion production (B), cell viability (C), intracellular ROS accumulation (D) and JNK phosphorylation (E) in Jurkat cells by KD548-Fc treatment. Cells were transfected with control siRNA or Nox1 siRNA for 36 hr and then incubated with KD548-Fc or TRAIL for the additional indicated periods (B, D, and E) or 40 hr (C) before the indicated assays. (B) The data are representative of three separate experiments with the same results. (B, D, E) Cells were treated with 0.8 μM of KD548-Fc. (B, E) 'Control' means untreated cells.
(C, D) Data represent mean ± SEM of three independent experiments carried out in triplicate. *, P <0.05; **, P <0.001 compared with the cells transfected with control siRNA.

Figure S5

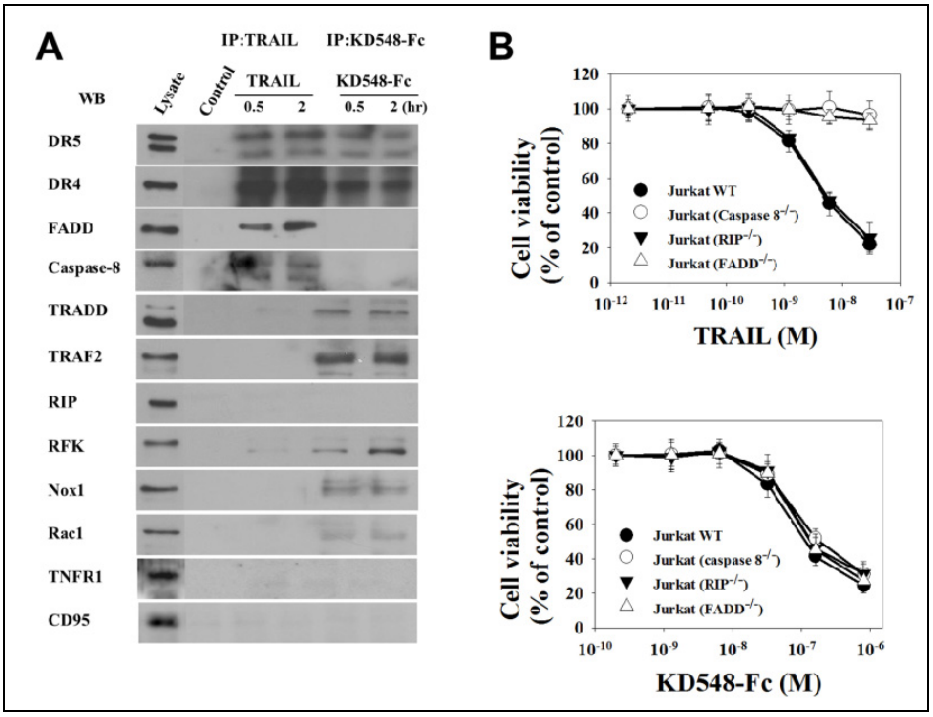

Figure S5. KD548-Fc induces a DR4/DR5-associated signaling complex composed of RFK, Nox1, Rac1, TRADD, and TRAF2, but not caspase-8, FADD or RIP1, distinct from the DISC induced by TRAIL in Jurkat cells.

(A) Western blots (WB) showing immunoprecipitation (IP) of the lysates of TRAIL- and KD548-Fc-treated cells using anti-FLAG antibody (for TRAIL) and anti-human Fc antibody (for KD548-Fc), respectively. Cells were left untreated (control) or treated with Flag-tagged TRAIL (30 nM) or KD548-Fc (0.8 μM) for 0.5 or 2 hr and then subjected to IP and/or WB.

(B) Cell viability of wild type, its FADD-deficient ($FADD^{-/-}$), caspase-8-deficient ($caspase\text{-}8^{-/-}$), or RIP-deficient ($RIP^{-/-}$) Jurkat cells, which were incubated with the indicated concentrations of TRAIL or KD548-Fc for 40 hr. Data represent mean ± SEM of three independent experiments carried out in triplicate.

Figure S6

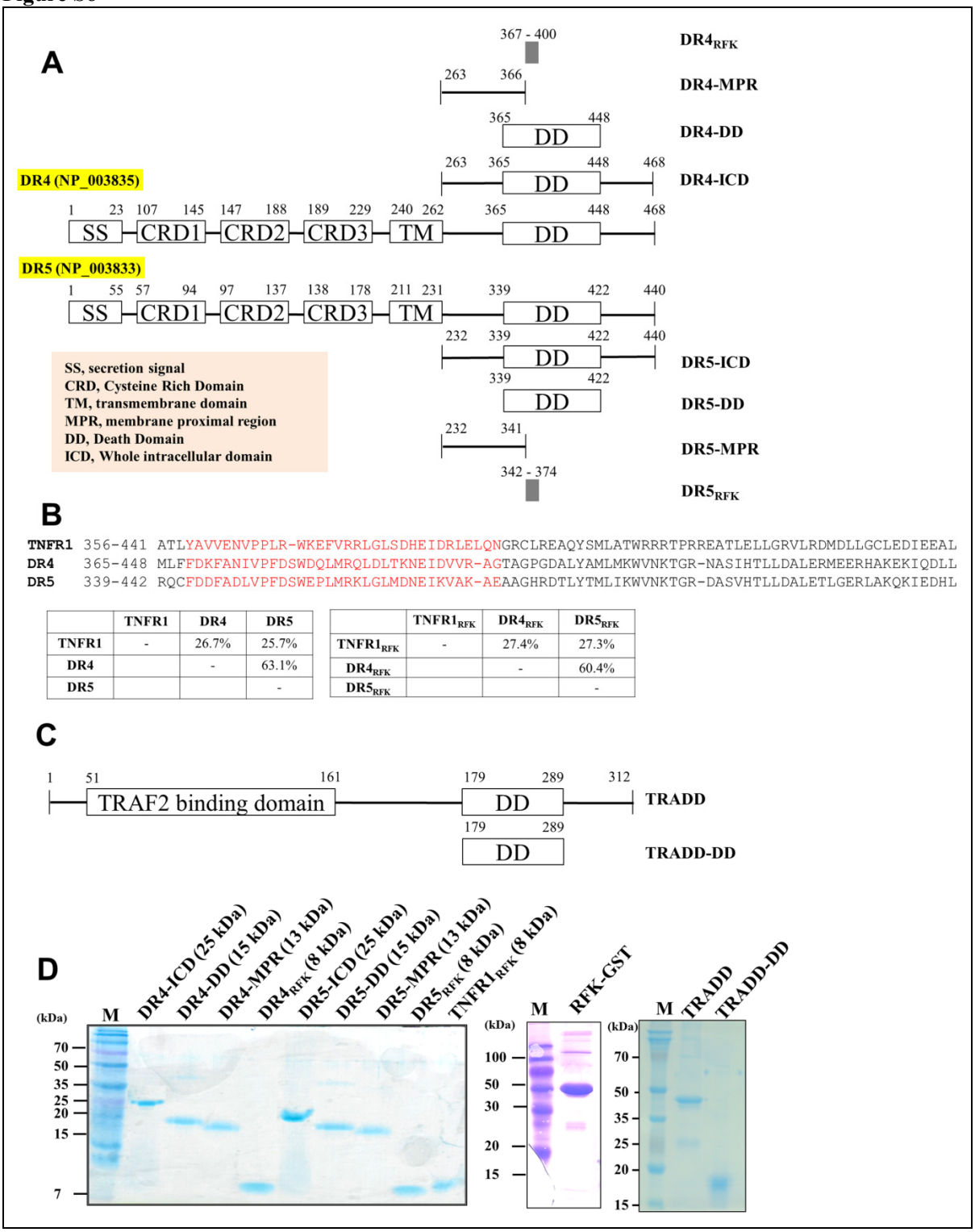

	TNFR1	DR4	DR5
TNFR1	-	26.7%	25.7%
DR4		-	63.1%
DR5			-

	TNFR1RFK	DR4RFK	DR5RFK
TNFR1RFK	-	27.4%	27.3%
DR4RFK		-	60.4%
DR5RFK			-

Figure S6. Determination of the intracellular regions of DR4 and DR5 responsible for the interaction with RFK or TRADD.

(A) Schematic representation of the whole organization of DR4 and DR5 proteins with highlights on the fragmentation of the intracellular regions of DR4 and DR5 to identify which regions are responsible for the interactions with RFK or TRADD. The whole intracellular region of DR4 (residues 263-468, DR4-ICR) and DR5 (residues 232-440, DR5-ICR) were divided into two domains: one is a membrane proximal region (MPR) before starting the DD, dubbed DR4-MPR (residues 263-366) and DR5-MPR (residues 232-341); the other is C-terminal region containing the DD, dubbed DR4-DD (residues 365-448) and DR5-DD (residues 339-422). The secretion signal sequence (SS), cysteine-rich domain (CRD), transmembrane domain (TM) and intracellular DD were highlighted in box. Numbers designate amino acids based on the following NCBI reference sequence, DR4 (NP_003835) and DR5 (NP_003833), with the initial methionine as residue 1. DR5 can be expressed in two distinct splice variants, long isoform of DR5B (440 residues) and short isoform of DR5A (411 residues) variants, which differ by presence and absence of 29 amino acids in the extracellular domain (185-213 residues) located between the CRD3 and the transmembrane domain (1).
(B) Sequence alignment of the DDs of DR4 and DR5 with the DD of TNFR1 to determine the potential RFK binding sites. Putative RFK binding sites within the DDs of DR4 and DR5 are shown in red. The tables show the sequence identity in percentage between the DDs (left) and RFK binding regions (right) of TNFR1, DR4, and DR5. The peptides, $DR4_{RFK}$ (residues 367-400) and $DR5_{RFK}$ (residues 342 -374), encompassing the putative RFK binding regions, were synthesized. Also, the peptide of $TNFR1_{RFK}$, harboring the RFK binding sites (residues 359-391) within the DD of TNFR1 (2,3), was synthesized.
(C) Schematic representation showing the whole organization of TRADD. The TRAF2 binding sites (residues 51 – 161) and DD (residues 179 – 289, TRADD-DD) are indicated (4,5).
(D) SDS-PAGE analyses of the purified proteins and synthesized peptides under reducing conditions. RFK was purified as C-terminal glutathione *S*-transferase fusion protein (RFK-GST) from *E. coli.* The purified proteins or synthesized peptides ($DR4_{RFK}$, $DR5_{RFK}$, and $TNFR1_{RFK}$) were separated on 15% (w/v) SDS-polyacrylamide gels under reducing conditions, and visualized by staining with Coomassie Blue R-250.

SUPPLEMENTAL EXPERIMENTAL PROCEDURES

Cell lines and reagents − HCT116 (colorectal carcinoma) cells were purchased from the ATCC (Manassas, VA) and grown in DMEM medium supplemented with 10% (v/v) FCS, 100 units/mL of penicillin, and 100 μg/mL streptomycin (Gibco Invitrogen) as described previously (6,7). Human T-cell leukemia Jurkat wild-type (A3 clone) and its mutant cell lines deficient in Rip1, caspase-8 (Jurkat I9.2), and FADD (Jurkat I2.1) were kindly provided by Prof. John Blenis (Dept. of Cell Biology, Harvard Medical School, MA, USA) (8) and cultured in RPMI1640 (WelGENE) supplemented with 10% (v/v) FCS, 100 units/ml of penicillin, and 100 μg/ml of streptomycin (Gibco Invitrogen) (9).

The following rabbit antibodies were used for Western blots: anti-caspase-3 was from Stressgen Inc.; anti-FADD was from Upstate Biotechnology; anti-phospho-JNK, anti-total-JNK, anti-poly(ADP-ribose) polymerase (PARP), anti-TRADD and anti-TRAF2 were from Cell Signaling Technology; anti-DR4 and anti-DR5 mAb was from Koma Biotech; anti-caspase-8 and anti-RIP1 were form BD Bioscience; anti-Nox1 was from Abcam; anti-Nox2 was from Novous; anti-Nox3, anti-Nox4, anti-Noxa1, and anti-Noxo1 were from Santa Cruz Biotech Inc.; anti-RFK was from Abnova Inc; anti-Rac1 was from Millipore; anti-β-actin was form Bethyl Laboratories Inc. Bovine serum albumin (BSA) was from Millipore. The soluble extracellular domains of TNFR1, TNFR2 and CD95 were from Invitrogen.

Protein expression and purification − The extracellular domains of DR4 (residues 106-239), DR5 (residues 52-183), DcR1 (residues 24-188), and DcR2 (residues 55-208) as well as soluble TRAIL (residues 114-281 with a C-terminal 6× His-tag) and TNFα (residues 77-233 with a C-terminal 6× His-tag) were expressed in *Escherichia coli* BL21 pLysS (DE3) and purified using anti-6×His Talon resin (Clontech), essentially as previously described (6,10). Flag-TRAIL (residues 114–281 with a C-terminal Flag tag) was expressed in *Escherichia coli* BL21 pLysS (DE3) and purified using anti-Flag M2 resin (Sigma) (6,10). The bacterial plasmid encoding RFK fused with glutathione S-transferase (GST) at the C-terminus, dubbed RFK-GST, was kindly provided from Prof. Martin Krönke (University of Cologne, Germany). RFK-GST was expressed in *E. coli* BL21 pLysS (DE3) and purified using glutathione-Sepharose 4B (GE Healthcare), as described previously (2). The purified proteins were sterilized by filtration using a cellulose acetate membrane filter (0.2 μm) (Nalgene Co.) before usages in cell assays.

The whole or partial regions of the intracellular domains of DR4 and DR5 and the whole (residues 1-312) or the DD (residues 179-289) of TRADD were respectively generated by PCR using the respective human cDNA (Invitrogen) as the template and subcloned into a bacterial cytosolic expression plasmid using *Nhe*I/*Bam*HI sites to be expressed with C-terminal 6×His-tagged proteins under the control of a T7 promoter. All of the constructs were confirmed by sequencing. Proteins were solubly expressed in the cytosol of *E.coli* and purified using anti-6× His Talon resin (Clontech), as described before (10). The peptides derived from the DDs of DR4 (amino acid residues 367-400, $DR4_{RFK}$), DR5 (amino acid residues 342-374, $DR5_{RFK}$), or TNFR1 (amino acid residues 331-363, $TNFR1_{RFK}$) were synthesized with N-terminal biotin (Peptron Inc.). Protein concentrations were determined using extinction coefficients calculated from the respective amino acid sequence and also confirmed by Bradford assay (Bio-Rad).

Binding analysis by ELISA − Binding specificity of KD548-Fc to the target proteins were determined by ELISA (6,10). ELISA plates (Nunc, Invitrogen Ltd.) were coated with 10 μg/ml of the extracellular domains of TNFR1, TNFR2, CD95, DR5, DR4, DcR1 or DcR2 for 2 hr at 37°C and blocked with 5% (w/v) bovine serum albumin (BSA) (Millipore). After washing with PBST (PBS plus 0.1% (v/v) Tween-20), KD548-Fc (1 μM), TRAIL (10 μg/ml) or TNFα (10 μg/ml) were applied to well for 1 hr at 25°C. After washing with PBST, bound proteins were detected with labeling of mouse anti-human Fc mAb (Sigma), anti-FLAG mAb (Sigma) or anti-His mAb (Ig Therapy) and then incubation with alkaline

phosphatase-conjugated goat anti-mouse mAb (Sigma). Absorbance was read at 405 nm on a VersaMax microplate reader (Molecular devices).

To determine the interactions of the intracellular regions of DR4 and DR5 with RFK-GST, TRADD, or TRADD-DD, the whole or partial fragments of the intracellular domains of DR4 or DR5 (10 μM) were coated overnight at 4°C and then RFK-GST (4 or 20 μM) or biotinylated-TRADD or –TRADD-DD (2 or 10 μM) were incubated at 25°C for 2 hr. The bound RFK-GST and biotinylated-TRADD or –TRADD-DD was detected with mouse anti-GST mAb (Upstate) and then alkaline phosphatase-conjugated goat anti-mouse mAb (Sigma) and alkaline phosphatase-conjugated goat anti-biotin mAb (Sigma), respectively, as described above.

For the interactions of TRADD or TRADD-DD with RFK-GST, TRADD or TRADD-DD (10 μM) was coated and then then various concentrations of RFK-GST were incubated at 25°C for 2 hr. The bound RFK-GST was detected as described above. For the interactions of DR4-DD or DR5-DD with TRADD-DD, DR4-DD or DR5-DD (10 μM) was coated and then then various concentrations of biotinlyated-TRADD-DD were incubated at 25°C for 2 hr. The bound biotinlyated-TRADD-DD was detected as described above. For the effects of TRADD-DD on the interactions between DR4-DD or DR5-DD and RFK, DR4-DD or DR5-DD (10 μM) was coated and then then various concentrations of RFK-GST were incubated in the absence or presence of TRADD-DD (10 μM) at 25°C for 2 hr. The bound RFK-GST was detected as described above. The binding raw data were normalized by setting BSA negative control as 0 and the maximal sample absorbance as 1 and then fitted into a four-parameter sigmoidal curve on Sigma plot software (SPSS Inc.) to estimate the apparent equilibrium dissociation constant (K_D) (10).

Competition ELISA − Competition ELISA between KD548-Fc and TRAIL for the binding to the extracellular domains of DR5 and DR4 was performed as described previously (10). Plates were coated with the extracellular domain of DR4 or DR5 (30 μg/ml) in PBS at 37°C for 1 hr and blocked with 5% (w/v) BSA. After incubations with various concentrations of KD548-Fc (0.1 nM - 1 μM) in the absence or presence of 1 μM TRAIL, the bound KD548-Fc was detected with alkaline phosphatase-conjugated goat anti-human Fc (Sigma), as described above.

For competitive ELISA between DR4-ICD or DR4-DD and $DR4_{RFK}$ or DR5-ICD or DR5-DD and $DR5_{RFK}$ for RFK binding, binding activity of $DR4_{RFK}$ (30 μM) and $DR5_{RFK}$ (30 μM) for plate-coated RFK-GST was assessed in the presence of serially diluted DR4-ICD or DR4-DD and DR5-ICD or DR5-DD, respectively. Then the bound biotinlyated-$DR4_{RFK}$ or -$DR5_{RFK}$ was detected by alkaline phosphatase-conjugated goat anti-biotin mAb as described above. For competitive ELISA between $DR4_{RFK}$ or $DR5_{RFK}$ and $TNFR1_{RFK}$ for RFK binding, plates were coated with $DR4_{RFK}$ (100 μM) or $DR5_{RFK}$ (100 μM) in PBS at 37°C for 1 hr and incubated with RFK-GST (10 μM) in the presence of serially diluted $TNFR1_{RFK}$ (200 μM ~ 0.1204 nM) at 37°C for 1 hr. Then the bound RFK-GST was detected as described above.

Cell viability assay − Cells seeded at density of 1×10^4 cells/well in 96-well plate were cultured overnight and treated with the indicated concentrations of KD548-Fc (0.8 μM -0.256 nM) or TRAIL (30 nM-0.096 nM) as specified in the Figure legends. Cell viability was analyzed using a colorimetric MTT (3-(4,5-dimethylthiazol-2-yl)-2,5-diphenyltetrazolium bromide)-based Cell Growth Determination kit (Sigma) (6,7). Then, the cell viability determined for at least triplicated experiments was presented as percentage of viable cells compared with untreated, control cells.

RNA interference − siRNA oligonucleotides were synthesized at Bioneer Co. The following siRNAs against DR4, DR5, TRADD, TRAF2, Nox1, Nox3 and Nox4 were used: DR4, 5′ -CAG ACU CGC UGU CCA CUU UUU-3′; DR5, 5′-UCA UGU AUC UAG AAG GUA A-3′; TRADD, 5′- GAA GAG CGC UGU UUG AAU U-3′; TRAF2, 5′- GUG UCG AGU CCC UUG CAG A-3′ and 5′- GGU CUU GGA

GAU GGA GGC A-3′; Nox1, 5′- GAA GGC CGA CAA AUA CUA C-3′ and 5′-GAA AAA UCC UUG GGU CAA C-3′; Nox3, 5′-CUC ACU UUC UGA GUU AUC A-3′; Nox4, 5′-CUG UUG UGG ACC CAA UUC A-3′ (2,6,11,12). Nox2 siRNA was purchased from Novous Inc. TNFR1 siRNA, Rac1 siRNA, Noxa1 siRNA, and Noxo1 siRNA were purchased from Santa Cruz Inc. An unrelated, scrambled siRNA with a sequence of 5′-AGA CAC ACG CAC UCG UCU C-3′ was employed as a control (6).

To evaluate effects of depletion of Nox1 - Nox4 siRNA, DR4, DR5, TNFR1, TRADD, or TRAF2 on the KD548-Fc- or TRAIL-induced cell death, superoxide anion generation, ROS production, and/or JNK phosphorylation, cells (5×10^5 cells/well in six-well plate or 1×10^4 cells/well in 96-well plate) were transfected with 2 μM of target-specific siRNA by electroporation in a 0.1-cm diameter capillary (Digital Biotech) (6,13) and then further incubated 36 hr prior to the following experiments.

Specific binding of KD548-Fc to cell surface-expressed DR4 and DR5 − Plasmids of T010 and T30 encoding DR5ΔCD-YFP fusion protein (the cytosolic domain deleted DR5 fused to yellow fluorescent proteins) and DR4ΔCD-YFP (the cytosolic domain deleted DR4 fused to yellow fluorescent proteins), respectively, were kindly provided by Prof. F.K. Chan (University of Massachusetts) (6,14). HeLa cells were transfected with the respective plasmid by electroporation (1,000 V and 1,500 AF) using a 0.1-cm diameter capillary (Digital Biotech, Korea), seeded at a density of 5×10^4 cells/well in 24-well plate over glass coverslips and grown for 30 hr. The cells were then washed once with PBS containing 3% (v/v) FCS and then stained with KD548-Fc (1 μM), Cetuximab (1 μg/ml), goat anti-DR5 antibody (1 μg/ml), goat anti-DR4 antibody (R&D System) for 30 min at 4°C. After three times washing with PBS containing 3% (v/v) FCS, cells were incubated with TRITC conjugated anti-human Fc (1:100) (sigma) or PE conjugated anti-goat Fc (1:100) (Abcam) in PBS for 1 hr at 4°C. The cells were then washed thrice with 3% (v/v) FCS and fixed using 4% (v/v) paraformaldehyde in PBS for 1 hr at 4°C. Images were obtained using a LMS510 model laser scanning confocal fluorescence microscope (LSM510; Carl Zeiss).

Caspase-8 and -3 activation assay − Caspase-8 or caspase-3 activity was measured using a colorimetric assay kit with the respective fluorogenic substrate (Thermo scientific) and then flow cytometry according to the manufacturer's protocol. Activity was normalized to untreated cells of the same type.

TUNEL assay − DeadEnd™ Fluorometric TUNEL system (Promega) was used to measure nuclear DNA fragmentation in apoptotic cells. Briefly, cells (1×10^4 cells/0.2 ml PBS) attached to microscope slide by cytospin were fixed with 4% (v/v) methanol-free formaldehyde in PBS for 25 min at 4°C, washed twice with PBS and treated with permeabilization solution (0.2% (v/v) Triton X-100 in PBS) for 5 min. After equilibration, cells were labeled with TdT reaction mix for 60 min at 37°C in the dark and then reaction was stopped by addition of 2×SSC (300 mM NaCl, 30 mM sodium citrate, pH 7.0). Cells were counterstained with Vectashield (mounting medium with DAPI, Vector Laboratories) and localized green fluorescence of apoptotic cells was detected by LMS510 model laser scanning confocal fluorescence microscope (LSM510; Carl Zeiss).

Annexin V and PI staining − For quantification of apoptosis, a FITC-conjugated annexin V and propidium iodide (PI) assay (BD Biosciences) was performed according to the manufacturer's instructions (7). Analysis of FITC and propidium iodide fluorescence intensities was performed with a FACS caliber flow cytometer. A total of 10,000 events/sample was acquired.

Surface Plasmon Resonance (SPR) − Kinetic parameters of the KD548-Fc with the DR4 and DR5, evaluated at 25°C using a Biacore 2000 biosensor (GE Healthcare). After immobilization of the extracellular domains of DR4 and DR5 onto the carboxymethylated dextran surface of a CM5 sensor chip at a density of approximately 400 response units (RUs), serially diluted KD548-Fc (25 nM - 400 nM) in

HBS-EP buffer (0.01 M HEPES pH 7.4, 0.15 M NaCl, 3 mM EDTA, 0.005 % (v/v) Surfactant P20) (GE healthcare) was injected into the flow cell at a flow rate of 30 μL/min for 2 min. BSA, as negative control, was also immobilized onto the carboxymethylated dextran surface of a CM5 sensor chip at a density of approximately 700 RUs and subjected to the above analysis. The dissociation (k_{off}) and association (k_{on}) rate constants, and the equilibrium dissociation constant (K_D) values, were determined by the bivalent analyte model using the BIAevaluation v3.2 software provided by the manufacturer.

SUPPLEMENTAL REFERENCES

1. Screaton, G. R., Mongkolsapaya, J., Xu, X. N., Cowper, A. E., McMichael, A. J., and Bell, J. I. (1997) *Curr. Biol.* **7**, 693-696
2. Yazdanpanah, B., Wiegmann, K., Tchikov, V., Krut, O., Pongratz, C., Schramm, M., Kleinridders, A., Wunderlich, T., Kashkar, H., Utermohlen, O., Bruning, J. C., Schutze, S., and Kronke, M. (2009) *Nature* **460**, 1159-1163
3. Adam-Klages, S., Adam, D., Wiegmann, K., Struve, S., Kolanus, W., Schneider-Mergener, J., and Kronke, M. (1996) *Cell* **86**, 937-947
4. Kieser, A. (2008) *Biol. Chem.* **389**, 1261-1271
5. Hsu, H., Shu, H. B., Pan, M. G., and Goeddel, D. V. (1996) *Cell* **84**, 299-308
6. Park, K. J., Lee, S. H., Kim, T. I., Lee, H. W., Lee, C. H., Kim, E. H., Jang, J. Y., Choi, K. S., Kwon, M. H., and Kim, Y. S. (2007) *Cancer Res.* **67**, 7327-7334
7. Sung, E. S., Kim, A., Park, J. S., Chung, J., Kwon, M. H., and Kim, Y. S. (2010) *Apoptosis* **15**, 1256-1269
8. Sprick, M. R., Weigand, M. A., Rieser, E., Rauch, C. T., Juo, P., Blenis, J., Krammer, P. H., and Walczak, H. (2000) *Immunity* **12**, 599-609
9. Park, K. J., Lee, S. H., Lee, C. H., Jang, J. Y., Chung, J., Kwon, M. H., and Kim, Y. S. (2009) *Biochem. Biophys. Res. Commun.* **382**, 726-729
10. Lee, C. H., Park, K. J., Sung, E. S., Kim, A., Choi, J. D., Kim, J. S., Kim, S. H., Kwon, M. H., and Kim, Y. S. (2010) *Proc. Natl. Acad. Sci. U S A* **107**, 9567-9571
11. Cheng, G., Cao, Z., Xu, X., van Meir, E. G., and Lambeth, J. D. (2001) *Gene* **269**, 131-140
12. Maranchie, J. K., and Zhan, Y. (2005) *Cancer Res.* **65**, 9190-9193
13. Sung, E. S., Park, K. J., Lee, S. H., Jang, Y. S., Park, S. K., Park, Y. H., Kwag, W. J., Kwon, M. H., and Kim, Y. S. (2009) *Mol. Cancer Ther.* **8**, 2276-2285
14. Clancy, L., Mruk, K., Archer, K., Woelfel, M., Mongkolsapaya, J., Screaton, G., Lenardo, M. J., and Chan, F. K. (2005) *Proc. Natl. Acad. Sci. U S A* **102**, 18099-18104